The influences of particle number on hot spots in strongly coupled metal nanoparticles chain

Z. B. Wang,[1,a)] B. S. Luk'yanchuk,[2] W. Guo,[1,3] S. P. Edwardson,[4] D. J. Whitehead,[1] L. Li,[1] Z. Liu,[3] and K. G. Watkins[4]

[1]*Laser Processing Research Centre, School of Mechanical, Aerospace and Civil Engineering, University of Manchester, Sackville Street, Manchester M60 1QD, United Kingdom*
[2]*Data Storage Institute, DSI Building, 5 Engineering Drive 1, Singapore 117608, Republic of Singapore*
[3]*Corrosion and Protection Centre, School of Materials, University of Manchester, The Mill, Manchester M60 1QD, United Kingdom*
[4]*Laser Group, Department of Engineering, University of Liverpool, Brownlow Street, Liverpool L69 3GH, United Kingdom*

In understanding of the hot spot phenomenon in single-molecule surface enhanced Raman scattering (SM-SERS), the electromagnetic field within the gaps of dimers (i.e., two particle systems) has attracted much interest as it provides significant field amplification over single isolated nanoparticles. In addition to the existing understanding of the dimer systems, we show in this paper that field enhancement within the gaps of a particle chain could maximize at a particle number $N > 2$, due to the near-field coupled plasmon resonance of the chain. This particle number effect was theoretically observed for the gold (Au) nanoparticles chain but not for the silver (Ag) chain. We attribute the reason to the different behaviors of the dissipative damping of gold and silver in the visible wavelength range. The reported effect can be utilized to design effective gold substrate for SM-SERS applications. © *2008 American Institute of Physics*. [DOI: 10.1063/1.2835598]

I. INTRODUCTION

Since single-molecule surface enhanced Raman scattering (SM-SERS) was reported,[1,2] it has attracted much attention and a number of studies have been devoted to investigate the mechanism of that.[3–6] Compared with conventional SERS (typical Raman enhancement factor of 10^6), SM-SERS detection requires much higher enhancement level that reaches around $10^{12}–10^{15}$.[1,6] Because of its very high sensitivity, SM-SERS is expected to have extensive applications in life science, medical science, environmental science, etc.[7]

To explain the giant field enhancement in SM-SERS, two main mechanisms have been proposed, namely, the electromagnetic mechanism and chemical mechanism. The electromagnetic mechanism has been understood primarily on the appearance of local hot spots in the gaps of a strongly coupled dimer (two metal nanoparticles, $N=2$) system or at the position near to the sharp tip of nonspherical (e.g., spheroid, square, and triangular) nanoparticles. The maximum peak enhancement predicted by the hot spot mechanism is around the order of 10^{11} for a dimer of truncated tetrahedron-shaped silver particles with a 1 nm gap.[4] It is below the nominal enhancement factor of SM-SERS of $10^{12}–10^{15}$,[1,2] and this is one reason why it is often thought that SM-SERS can only be observed for resonant Raman scatters where chemical charge-transfer mechanism is assumed to produce additional enhancement by a factor of 10^2 or more.[4,6] Very

recently, it was demonstrated that a purely electromagnetic mechanism for SM-SERS is possible for a solid/nanoshell silver dimer array (enhancement factor larger than 10^{13}) by combining the strong near-field coupling effect within an isolated dimer and long-range photonic interaction of widely spaced dimers.[8] In the majority of these studies, the focused modeling system is a dimer which consists of two particles (or an array of widely spaced dimers), possibly because it is the simplest system for representing aggregates and is easier for theoretical treatment than more particles. Although it is known that hot spots also exist in particle chains[1,9] (for example, Stockman's group reported giant multiplicative enhancement for linear chains of metal nanoparticles with progressively decreasing gaps and particle sizes[5]), it is, however, not clear what the differences are between the hot spots in a dimer system and in a chained system containing different numbers of same sized particles, and it is also not known whether dimer is the best optimized system to produce highest possible enhancement in the gap region for SM-SERS applications. In this paper, we have carried out numerical studies on the wavelength-dependent peak enhancement evolution in the gaps of a nanoparticle chain system, with the particle number varying from 1 to infinity. We have found that the enhancement in the gaps of the particle chain, indeed, depends on the particle number and could reach its maximum at a different number, depending on the optical properties of the particles. Moreover, the resonance peaks are also redshifted with increasing particle number. These effects are expected to find important applications in designing highly effective SM-SERS-active substrates.

---

a)Author to whom correspondence should be addressed. Electronic mail: zengbo.wang@gmail.com.

128, 094705-1

II. FINITE INTEGRATION TECHNIQUE (FIT) AND SIMULATIONS

Although it was discovered nearly a century ago, Mie theory continues to play a crucial role in describing the optical properties of metal nanoparticles, especially spherical gold and silver nanoparticles.[10] Many basic effects, such as redshift and broadening of dipole resonance and appearance of high-order (quadruple and octapole) resonance modes as particle size increases, can be understood within this theory. However, Mie theory cannot be directly applied to describe the electrodynamics of nanoparticles with arbitrary shapes, degree of aggregation, and complex external dielectric environments. To meet these needs, several new computational techniques have been developed over the last 30 years.[11] It includes semianalytical methods such as multiple multipole technique,[12] discrete dipole approximation,[13] dyadic Green function technique,[14] and pure numerical methods such as finite element method (FEM),[15] finite difference time domain (FDTD) technique,[16] and finite integral technique (FIT).[17] The FIT technique, proposed by Weiland,[17] provides a universal spatial discretization scheme, applicable to various electromagnetic problems, ranging from static field calculations to high frequency applications in time or frequency domain. Unlike most numerical methods, FIT discretizes Maxwell's equation in an integral form rather than the differential ones. In the case of Cartesian grids, the FIT formulation can be rewritten in time domain to yield standard FDTD methods. While in the case of triangular grids, the FIT has tight links with FEM methods formulated in Whitney forms.[18] In this paper, a commercial FIT software package [CST MICROWAVE STUDIO 2006 (Ref. 19)] was used. For better accuracy on simulation results, we have chosen to use triangular grids (thus a FEM-like method in this paper), which are naturally conformal to the circular boundary of a sphere. Each particle within the chain was discretized by tetrahedral meshes with a maximum edge length of $a/5$, where a is the particle radius. The incident wave is a linearly polarized plane wave with electric vector directed along the particle chain. The desired linear equation system solver accuracy in terms of the relative residual norm was set as 10^{-6}, which enforce a termination criterion for each solver run at a single wavelength sample. The retardation effect and contributions from all necessary orders of partial waves (dipole, quadruple, etc.) are inheritably considered in our modeling. The calculations were performed on a 64 bit workstation with 16 GB memory and two 3.2 GHz CPUs.

The wavelength-dependent dielectric constant used in the calculations, $\varepsilon(\lambda) = \varepsilon'(\lambda) + i\varepsilon''(\lambda)$, was directly taken from the bulk experimental data in Palik's book.[20] It means that we are not including nonlocal or size dependent dielectric response for small particles whose diameter is close to the bulk electron mean free path (size effect is significant for particle diameter less than 5 nm).[21] In that case, electron scattering at the particle boundary becomes a dominant effect, and it leads to the increase of dissipative damping factor $\varepsilon''(\lambda)$. To make this effect negligible, we have limited par-
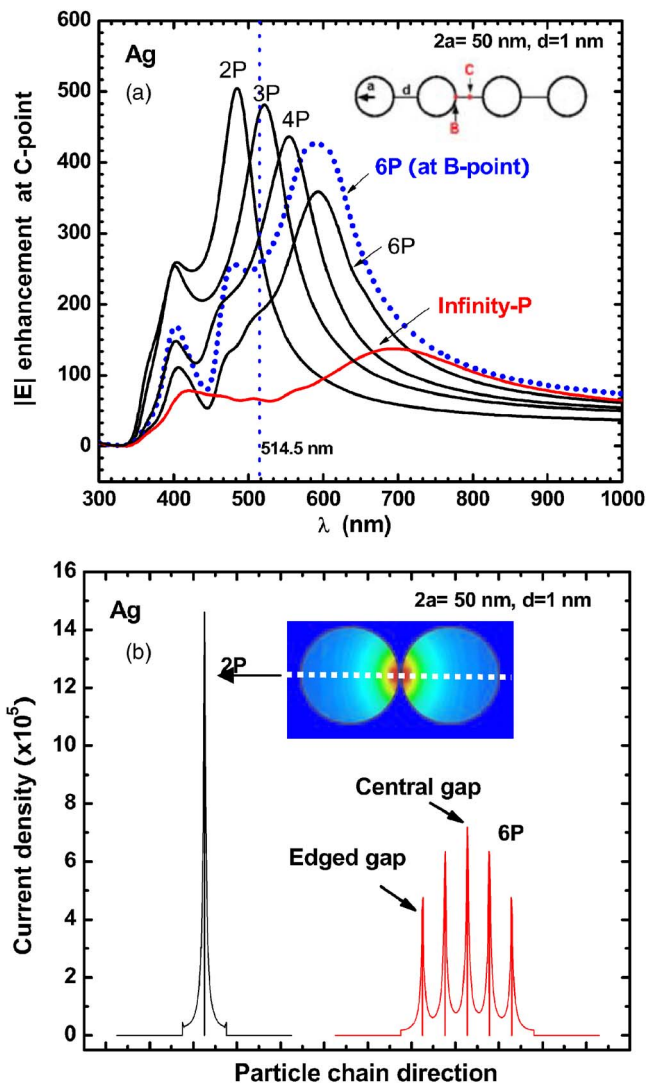
FIG. 1. (Color online) (a) $|E|$ enhancement at the middle of the central gap (hot spot C as in inset) in a silver nanoparticle chain with different numbers N of 50 nm particles, as a function of wavelengths. Also shown is the maximum enhancement on the particle surface for $N=6$ particle chain. (b) Corresponding current density distribution across the particle chain centers for $N=2$ and $N=6$ particle chains.

ticle diameter to be not smaller than 40 nm in our simulations. Meanwhile, we limited our investigation on particles in spherical shape.

III. RESULTS AND DISCUSSIONS

Figure 1 shows the calculated local amplitude enhancement of the electric field, $|E|$, at the middle of the central gap [hot spot C as in the inset drawing of Fig. 1(a)] in a 50 nm silver nanoparticle chain, with close spacing $d=1$ nm. Two distinct resonance modes can be observed for each solid curve in Fig. 1(a): main resonance peaks associated with coupled plasmon mode within the chain and minor resonance peaks associated with dipole resonance of each single particle. As particle number N increases, both the dipole resonance peaks and the main resonance peaks are redshifted and broadened. However, the tendencies are much more pronounced for the main resonances, as the peak shifts from 480 nm for $N=2$ to 590 nm for $N=6$. The dipole peaks are

located at a wavelength of around 400 nm (single silver particle resonance peak is at 370 nm) and its redshifting is almost negligible. Meanwhile, their $|E|$ enhancements are much lower than the main resonance peaks, indicating the dominant role of coupled plasmon modes in the chain. These coupled plasmon modes are caused by the Coulomb attraction between the opposite polarization charges on both sides of the gap. In a dimer system, the Coulomb attraction concentrates those charges at the surface points closest to each other, thus greatly enhances the fields in the region between them. As it can be seen in Fig. 1(a), in the silver dimer the maximum $|E|$ enhancement ($|E|_{max}$) reaches around 500 (Raman $|E|^4 \sim 6.25 \times 10^{10}$), when it was excited by a 480 nm laser line. The $|E|_{max}$ at hot spot C decreases with increasing N, dropping to 360 at $N=6$ and further dropping to 137 when N becomes infinity. In Fig. 1(b), the corresponding current density distributions across the chain centers were given for $N=2$ and $N=6$. It clearly shows that a smaller current density is induced within the $N=6$ particle chain compared to the $N=2$ dimer system. In the $N=6$ chain, it is observed that current density is highest near the central gap region, and lowest near the edged gap region [see markings in Fig. 1(b)]. In other words, the electric field is mostly enhanced in the central gap compared to other gaps. For the field inside the central gap, we found that the distribution of $|E|$ along the BC line [see inset drawing in Fig. 1(a) for this line] is almost uniform for small numbered systems such as dimer ($N=2$) and trimer ($N=3$), but it is not the case for larger numbered systems. The enhancement at points B and C starts to deviate at $N=4$, and the difference increases slowly with N. The maximum difference is around 170 for an infinity N. The example demonstrating field difference at points B and C is also shown in Fig. 1(a), by the dashed line for the case $N=6$. A new minor peak appears at 490 nm, which can be seen as a sign of the contribution from higher order multipoles. The higher enhancement obtained at hot spot B for $N \geqslant 4$ particle chain, however, never exceeds the values of peak enhancement at $N=2$. Therefore, we can conclude that, for silver nanoparticles, the dimer is indeed the best optimized system for achieving highest possible enhancement at the gap center if an appropriate excitation laser is used. At a wavelength of 514.5 nm, which was commonly used for silver-based SERS Raman spectroscopy, $|E|$ enhancement at hot spot C is almost the same to be 300 (Raman $|E|^4 \sim 8.1 \times 10^9$) for $N=2$ and $N=4$, and reaches a maximum $|E|$ enhancement of 420 at $N=3$ [see vertical dashed mark line in Fig. 1(a)].

In comparison with silver nanoparticle chain, the $|E|$ enhancement at hot spot C among a gold nanoparticle chain has a similar redshift tendency of the resonance wavelengths on increasing N, but shows different behaviors on peak maxima and spectrum shapes, as shown in Fig. 2. Most interestingly, the highest possible $|E|$ enhancement is now seen for $N=8$ ($|E|_{max}=470$) instead of $N=2$ ($|E|_{max}=140$). In other words, a gold dimer system is not the best aggregation state for producing maximum field enhancement in the central gap of the chain. The resonance peaks and enhancement peak values for different particle numbers N were extracted from Fig. 2(a) and shown in Fig. 2(b). As can be seen when $N<8$, increas-
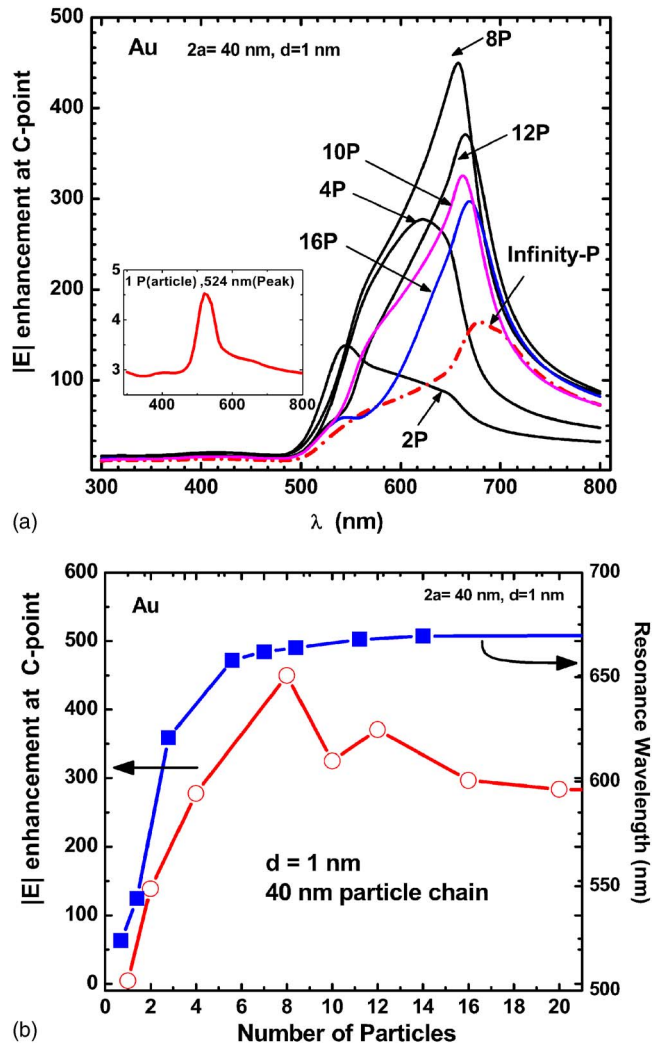
FIG. 2. (Color online) (a) $|E|$ enhancement at hot spot C in a gold nanoparticles chain with different numbers of same sized particles, as a function of wavelengths. (b) presents the corresponding peak enhancement value and resonance wavelength extracted from (a).

ing the particle number N leads to a higher field enhancement. The situation is slightly more complicated for the $8 \leqslant N \leqslant 12$ chains. The field enhancement peak drops from 470 to 335 when N increases from 8 to 10, but it rebounds back to 374 when N increases further to 12. At particle number $N>12$, field enhancement gradually drops, approaching a value of 167 at an infinity number. In addition, one can see from Fig. 2(a) that the spectrum shapes are rather asymmetrical with respect to the main resonance peaks. Meanwhile, the minor peaks associated with dipole resonances, which are clearly seen for silver chain as in Fig. 1(a), becomes undistinguishable for $N \geqslant 2$ gold chain. Figure 3 presents the corresponding $|E|$-field distribution in the equatorial plane of the eight-particle chain that maximizes the field in the central gap, as shown in Fig. 2. We can see that the field in the central gap differs clearly from those in other gaps. It has a prolonged field profile along the direction perpendicular to the particle chain and a higher enhancement amplitude. Moreover, the highest field enhancement within the central gap region was identified, not located on the shortest line liking two particle centers, but on some other position near to
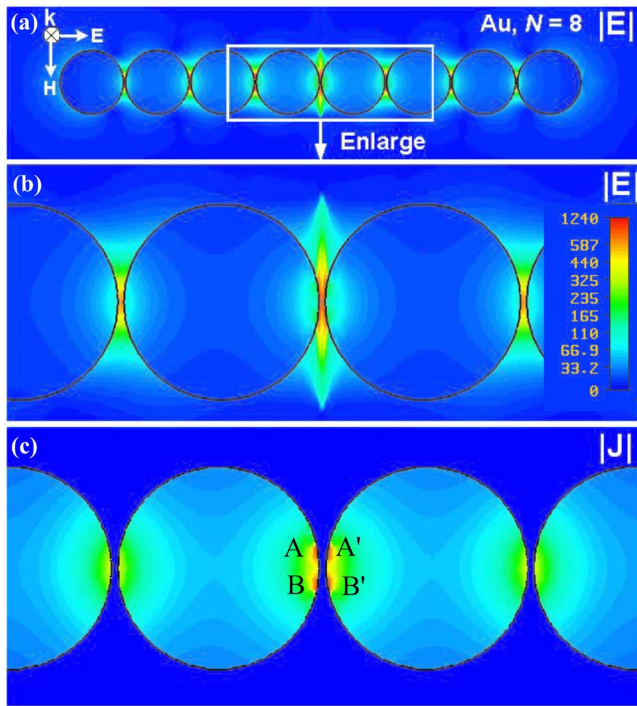
FIG. 3. (Color online) (a) $|E|$-field distribution in the plane across centers of eight 40 nm sized nanoparticles, arranged in a linear chain with a close spacing of 1 nm. (b) and (c) show the enlarged view of field and current density around central gap region, respectively.

it. In present case, we have found a highest field enhancement of 1240 within the central gap region, which means a Raman enhancement up to 2.4×10^{12}. Such a high Raman enhancement level has never been reported for gold aggregates consisting of pure spherical-shaped nanoparticles. We thus expect that the reported effect would find its important applications in designing highly efficient gold-base SM-SERS-active substrates. The origin of the nonuniform field within the central gap can, again, be understood on the picture of the current density distribution, as shown in Fig. 3(c). The coupled plasmon modes in the chain leads to the generation of two charge confinement centers in each of the centered particles [see marks A-A' and B-B' in Fig. 3(c)]. The Coulomb attraction between the opposite polarization charges on both sides of the central gap can take place between A-A', A-B', B-A', and B-B'. The final field distribution is a total effect of all these Coulomb interactions.

For a linear chain with N particles, the total length including the spacing gaps is

$$\ell = N \cdot (2a) + (N-1) \cdot d, \tag{1}$$

where a is the particle radius and d the spacing distance. At $N=8$, the total length of the chain is $\ell=327$ nm. Compared with the resonance wavelength [$\lambda_{\text{res}}=658$ nm as in Fig. 2(b)] for the $N=8$ gold chain, one easily finds the following relationship:

$$\ell \cong \lambda_{\text{res}}/2, \tag{2}$$

which is exactly the well-known equation for a $\lambda/2$ dipolar antenna in classical radiowave antenna theory. This effect was not observed for silver chain as in Fig. 1(a). By combin-

ing Eqs. (1) and (2), we obtain an optimal particle number N_{opt} for achieving highest possible field enhancement in the central gap:

$$N_{\text{opt}} \cong \frac{2d + \lambda_{\text{res}}}{2(2a + d)}. \tag{3}$$

In the cases that particle spacing is much smaller than particle radius ($d \ll a$), Eq. (3) reduces to

$$N_{\text{opt}} \approx \frac{\lambda_{\text{res}}}{4a}. \tag{4}$$

The validity of Eq. (4) was confirmed for gold nanoparticles chain with different particle sizes at a fixed spacing $d=1$ nm. For example, we found $N_{\text{opt}} \approx 5$ for 80 nm particle chain ($\lambda_{\text{res}}=730$ nm, $|E|_{\text{max}}=378$) and $N_{\text{opt}} \approx 2$ for 160 nm chain ($\lambda_{\text{res}}=650$ nm, $|E|_{\text{max}}=370$). As the particle size increases, peak enhancement $|E|_{\text{max}}$ always drops. This is due to the stronger radiation damping process in larger particles.[22] When particle size exceeds 160 nm, we found that gold dimer is always the best system for highest possible enhancement in the gap, which is similar to the case of 50 nm sized silver chains in Fig. 1(a). A little bit of disorder (such as some particles are slightly shifted from the chain axis and inhomogeneous spacing) in the chain does not affect the validity of Eq. (4), and can even increase the magnitude of field peak. It is necessary to point out that, although the optimal $\lambda/2$ length works for the hot spots problem in strongly coupled gold chains [as in Eq. (2)], optical antennas made from gold nanowires or strips do not often resonate at a length corresponding to one-half of the incident wavelength, and usually the optimal length is considerably shorter than the half wavelength.[23]

To explain why the particle number effect was only theoretically observed for gold nanoparticles chain but not for silver nanoparticle chain, we have paid our attention to the different damping behaviors of gold and silver in the investigated spectral range. It is well known that plasmon resonance-induced field enhancement near small metal nanoparticles is limited by the damping processes, which include radiation damping and dissipative (electron relaxation) damping.[24] Radiation damping is an inhabit process associated with particle plasmon resonances. It has no direct links with dissipative factor $\varepsilon''(\lambda)$, and can happen even when $\varepsilon''(\lambda)$ is zero. We have shown in a series of recent papers that peculiarities (anti-Rayleigh hierarchy scattering) arise in the light scattering by isolated small nanoparticles and nanowires near their plasmon resonance wavelengths, when the dissipative factor $\varepsilon''(\lambda)$ is low enough and radiation damping prevails the dissipative damping.[25] In the wavelength regime for gold within 655–1000 nm and silver within 350–750 nm (see Fig. 4), the material properties can be well described by the Drude–Sommerfeld model. It implies a free-electron-like oscillation behavior inside metals within these wavelength ranges and the corresponding dissipative damping process can be described by a fixed damping rate. For silver nanoparticle chain as in Fig. 1(a), resonance wavelengths for different particle numbers N are lying within the above wavelength range and thus one can consider that the dissipative
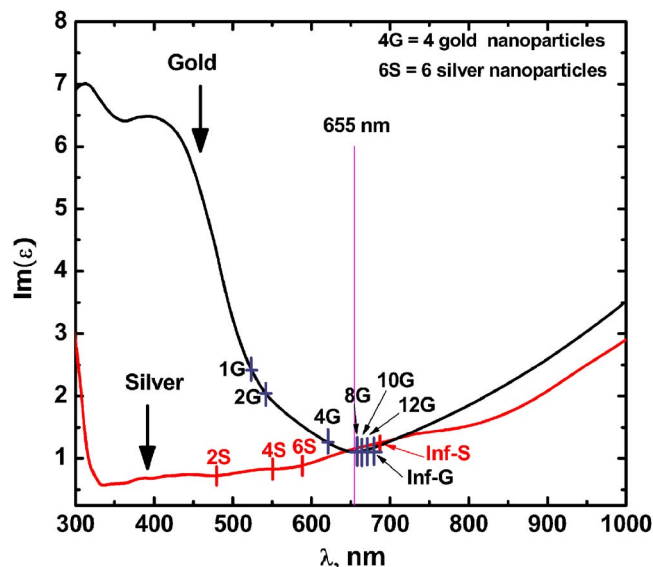
FIG. 4. (Color online) Imaginary part of the used dielectric constants for gold and silver in a wavelength range from 300 and 1000 nm.

damping process in the chain remains at same level. The dropping of the peak enhancement for silver chain with increasing particle number N should be related to the enhanced radiation damping process, as evidenced by the homogenous broadening of spectrum in Fig. 1(a). Unlike silver, gold manifests much higher dissipative damping at wavelengths below 655 nm, due to the excitation of interband transitions. Noting that the resonance wavelengths of gold as shown in Fig. 2 fall into this regime, the dissipative damping in gold is thus more pronounced than that in silver. Due to the mediation of this dissipative damping process, field enhancement maximizes at around 655 nm for eight-particle chain when gold has a minimum dissipative factor. Moreover, the spectrum becomes asymmetrical which can be thought as the total effect of the two damping processes with competitive contributions. It is important to remember that we only studied ordered spherical particles chain in this paper and particle chain consisting of other-shaped particles could produce best optimized hot spots at different particle numbers, as given by Eqs. (3) and (4).

As a final note, we would like to point out that the proposed metal nanoparticles chain with limited particle number can be fabricated with E-beam lithography technique, or optical tweezers by moving nanoparticles into near-field contact with other particles, as was recently demonstrated by Svederg et al.[26] It is also possible to use atomic force microscope tip to move the particles into chain arrangement.[27]

IV. SUMMARY

We have investigated the hot spots within a metal particle chain with varying particle number. It was shown that the field enhancement in the central gap is higher than other gaps, and it can maximize at a particle number larger than 2. This means that the dimer system was not always the best system for achieving the highest possible field enhancement in the gaps for SM-SERS applications. The effect, however, was only observed for gold chain but not for silver chain, due to the stronger dissipative damping processes at resonance wavelengths smaller than 655 nm.

[1] S. Nie and S. R. Emmony, Science **275**, 1102 (1997).
[2] K. Kneipp, Y. Wang, H. Kneipp, L. T. Perelman, I. Itzkan, R. R. Dasari, and M. S. Feld, Phys. Rev. Lett. **78**, 1667 (1997).
[3] E. C. Le Ru, P. G. Etchegoin, and M. Meyer, J. Chem. Phys. **125**, 204701 (2006); K. Imura, H. Okamoto, M. K. Hossain, and M. Kitajima, Nano Lett. **6**, 2173 (2006).
[4] E. Hao and G. C. Schatz, J. Chem. Phys. **120**, 357 (2004).
[5] K. Li, M. I. Stockman, and D. J. Bergman, Phys. Rev. Lett. **91**, 227402 (2003).
[6] H. X. Xu, J. Aizpurua, M. Kall, and P. Apell, Phys. Rev. E **62**, 4318 (2000).
[7] M. Moskovits, Rev. Mod. Phys. **57**, 783 (1985).
[8] S. L. Zou and G. C. Schatz, Chem. Phys. Lett. **403**, 62 (2005); K. Zhao, H. X. Xu, B. H. Gu, and Z. Y. Zhang, J. Chem. Phys. **125**, 081102 (2006).
[9] F. J. Garcia Vidal and J. B. Pendry, Phys. Rev. Lett. **77**, 1163 (1996).
[10] G. Mie, Ann. Phys. **25**, 377 (1908).
[11] L. Novotny and B. Hecht, *Principles of Nano-Optics* (Cambridge University Press, Cambridge, 2006).
[12] C. Hafner, *The Generalized Multiple Multipole Technique for Computational Electromagnetics* (Artech, Boston, 1990).
[13] W. H. Yang, G. C. Schatz, and R. P. Vanduyne, J. Chem. Phys. **103**, 869 (1995).
[14] O. J. F. Martin, C. Girard, and A. Dereux, Phys. Rev. Lett. **74**, 526 (1995).
[15] J. M. Jin, *The Finite Element Method in Electromagnetics*, 2nd ed. (Wiley, New York, 2002).
[16] *Computational Electrodynamics: The Finite-Difference Time-Domain Method*, edited by A. Taflove (Artech House, Boston, 2005).
[17] T. Weiland, Int. J. Numer. Model. **9**, 295 (1996).
[18] U. V. Rienen, *Numerical Methods in Computational Electrodynamics. Linear Systems in Practical Applications* (Springer, Berlin, 2001).
[19] Computer Simulation Technology, CST MICROWAVE STUDIO, http://www.cst.com; remote license access provided by one of the author B. S. Lukiyanchuk in DSI, Singapore, 2007.
[20] *Handbook of Optical Constants of Solids III*, edited by E. D. Palik (Academic, New York, 1998).
[21] *Optical Properties of Metal Clusters*, edited by U. Kreibig and M. Vollmer (Springer-Verlag, Berlin, 1995).
[22] A. Melikyan and H. Minassian, Appl. Phys. B: Lasers Opt. **78**, 453 (2004).
[23] R. Kappeler, D. Erni, X. D. Cui, and L. Novotny, J. Comput. Theor. Nanosci. **4**, 686 (2007); P. Muhlschlegel, H. J. Eisler, O. J. F. Martin, B. Hecht, and D. W. Pohl, Science **308**, 1607 (2005).
[24] C. Sonnichsen, T. Franzl, T. Wilk, G. von Plessen, J. Feldmann, O. Wilson, and P. Mulvaney, Phys. Rev. Lett. **88**, 077402 (2002).
[25] B. S. Luk'yanchuk, M. I. Tribelsky, Z. B. Wang, Y. Zhou, M. H. Hong, L. P. Shi, and T. C. Chong, Appl. Phys. A: Mater. Sci. Process. **89**, 259 (2007); B. S. Luk'yanchuk, M. I. Tribelsky, V. Ternovsky, Z. B. Wang, M. H. Hong, L. P. Shi, and T. C. Chong, J. Opt. A, Pure Appl. Opt. **9**(9), S294 (2007); Z. B. Wang, B. S. Luk'yanchuk, M. H. Hong, Y. Lin, and T. C. Chong, Phys. Rev. B **70**, 035418 (2004).
[26] F. Svedberg, Z. P. Li, H. X. Xu, and M. Kall, Nano Lett. **6**, 2639 (2006).
[27] R. Resch, C. Baur, A. Bugacov, B. E. Koel, A. Madhukar, A. A. G. Requicha, and P. Will, Langmuir **14**, 6613 (1998).
[28] http://www.nwlec.org.uk.